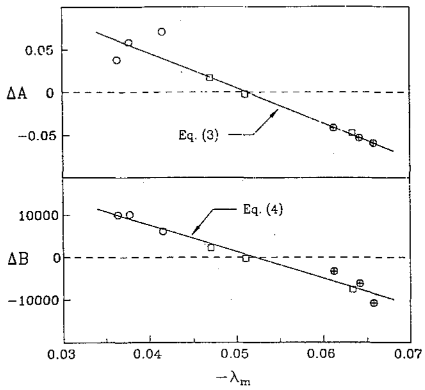


**Fig. 2 Variation of $A$ and $B$ against the mean Thwaites parameter; see Fig. 1 for legend.**

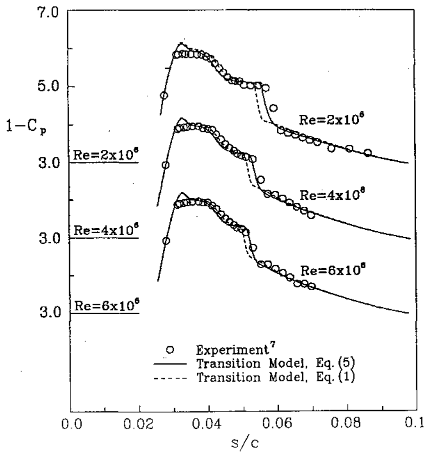


**Fig. 3 Pressure distributions on the modified NACA 0010 section at $\alpha$ = 8 deg for various Reynolds numbers.**

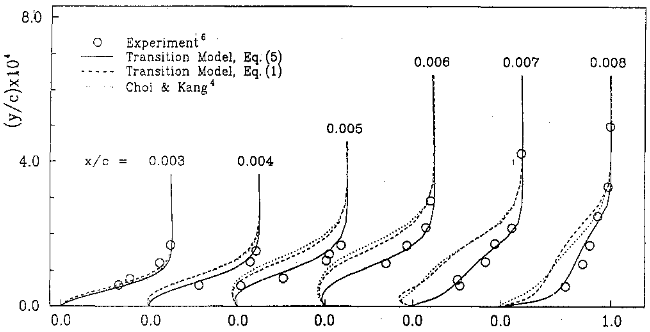


**Fig. 4 Comparison of velocity profiles on the NACA 63-009 section for $Re$ = 5.8 × 10$^6$ at $\alpha$ = 7 deg.**

procedure resembles the two-step transition prediction of Granville for the attached flow.

To verify this new transition model, the calculations have been repeated for the modified NACA 0010 and the NACA 63-009 sections. Figure 3 compares the pressure distributions for the modified NACA 0010 section at $\alpha = 8$ deg for various Reynolds numbers. The results using the new transition model, Eq. (5), are seen to be in good agreement, whereas those using the correlation without the coefficient correction, i.e., Eq. (1), exhibit considerable departure from the data in the pressure recovery region. The discrepancy is attributable to the difference in transition locations. For $\alpha = 12$ deg, the pressure distributions (not shown) using Eq. (5) were found to be in similarly good agreement with the data whereas the calculation with Eq. (1) failed to yield a converged solution. What has been shown is that the corrections made to the coefficients improved the performance substantially, although Eqs. (3) and (4) do not exactly fit the $\Delta A$ and $\Delta B$ data as seen in Fig. 2 (open circles).

The velocity profiles at various sections for $Re = 5.8 \times 10^6$ and $\alpha = 7$ deg are compared in Fig. 4. The figure, which shows the results by Eqs. (1) and (5) and the earlier results by Choi and Kang,[4] emphasizes the importance of the correct transition location for the successful analysis of the transitional separation bubble. Even when the pressure distributions seem to be in reasonable agreement, the velocity profiles could be entirely different. Among many correlations, only Eq. (5) gives a correct prediction whereas the other formulas grossly overpredict the bubble.

## Summary

The two-layer $k$–$\varepsilon$ turbulence models has been incorporated successfully in the Navier–Stokes procedure developed earlier to solve the transitional separation bubble on an airfoil. On the basis of the transition points deduced from a series of calculations with this improved procedure, a new transition criterion for leading-edge separation bubbles that correlates the transition Reynolds number with the Reynolds number at separation and the Thwaites parameter is established. Sample calculations demonstrate that this correlation performs excellently for all of the cases examined.

## References

[1]Kwon, O. K., and Pletcher, R. H., "Prediction of Subsonic Separation Bubbles on Airfoils by Viscous-Inviscid Interaction," *Numerical and Physical Aspects of Aerodynamic Flows II*, edited by T. Cebeci, Springer–Verlag, New York, 1984, pp. 193–204.

[2]Vatsa, V. N., and Carter, J. E., "Analysis of Airfoil Leading-Edge Separation Bubbles," *AIAA Journal*, Vol. 22, No. 12, 1984, pp. 1697–1704.

[3]Cebeci, T., "Essential Ingredients of a Method for Low Reynolds-Number Airfoils," *AIAA Journal*, Vol. 27, No. 12, 1989, pp. 1680–1688.

[4]Choi, D. H., and Kang, D. J., "Calculation of Separation Bubbles Using a Partially Parabolized Navier–Stokes Procedure," *AIAA Journal*, Vol. 29, No. 8, 1991, pp. 1266–1272.

[5]Chen, H. C., and Patel, V. C., "Near-Wall Turbulence Models for Complex Flows Including Separation," *AIAA Journal*, Vol. 26, No. 6, 1988, pp. 641–648.

[6]Gault, D. E., "Boundary-Layer and Stalling Characteristics of the NACA 63-009 Airfoil Section," NACA TN 1894, June 1949.

[7]Gault, D. E., "An Experimental Investigation of Regions of Separated Laminar Flow," NACA TN 3505, Sept. 1955.

# Two-Equation Model for Turbulent Wall Flow

Michael M. Gibson* and Adil A. Dafa'Alla†
*Imperial College of Science, Technology and Medicine, London SW7 2BX, England, United Kingdom*

## Introduction

THE trouble with the $k$-$\varepsilon$ turbulence model is that neither of the equations is well adapted to integration through the viscous layers to the wall. The purpose of the present paper is to show how some of the difficulties may be alleviated by the choice of alternative variables.

In the usual form of the $k$-$\varepsilon$ model the eddy viscosity is defined by

$$\nu_t = C_\mu f_\mu (k^2/\varepsilon) \qquad (1)$$

with $k$ the turbulent kinetic energy and $\varepsilon$ its dissipation rate obtained from the equations

$$U_i \frac{\partial k}{\partial x_i} = \frac{\partial}{\partial x_j}\left\{\left(\nu + \frac{\nu_t}{\sigma_k}\right)\frac{\partial k}{\partial x_j}\right\} + P - \varepsilon \qquad (2)$$

Received July 20, 1994; revision received Oct. 6, 1994; accepted for publication Oct. 7, 1994. 

*Reader, Mechanical Engineering Department, Exhibition Road.

†Research Associate, Mechanical Engineering Department, Exhibition Road.

$$U_i\frac{\partial\varepsilon}{\partial x_i}=\frac{\partial}{\partial x_j}\left\{\left(\nu+\frac{\nu_t}{\sigma_\varepsilon}\right)\frac{\partial\varepsilon}{\partial x_j}\right\}+C_{\varepsilon1}f_{\varepsilon1}\frac{\varepsilon}{k}P$$
$$-C_{\varepsilon2}f_{\varepsilon2}\frac{\varepsilon^2}{k}+\psi+\xi \tag{3}$$

$P\equiv-\overline{u_iu_j}\partial U_i/\partial x_j$ is the rate of production of $k$ from the mean flow, and $\psi$ and $\xi$ stand for terms added to the $\varepsilon$ equation by various authors to account in a variety of ways for additional production by mean shear and to achieve correct limiting behavior very close to a wall, where viscous diffusion of $\varepsilon$ balances the dissipation. The model constants $C_\mu$, $C_{\varepsilon1}$, $C_{\varepsilon2}$, $\sigma_k$, and $\sigma_\varepsilon$ have long been established for high-Reynolds-number conditions: $C_{\varepsilon2}$ by reference to the observed rate of decay of grid turbulence, $C_\mu$ chosen to give $\overline{uv}/k\approx-0.3$ in local-equilibrium shear flow, with a relationship between the remaining constants derived from the law of the wall. A variety of damping functions $f_\mu$, $f_{\varepsilon1}$, and $f_{\varepsilon2}$ have been used to account for viscous effects in the sublayers where the turbulence Reynolds number approaches zero.

It is in this area that the deficiencies of the $k$-$\varepsilon$ model become apparent. A fine grid is needed to resolve the small-scale motion near the wall where large changes in $k$ and $\varepsilon$ occur, and the lack of a natural boundary condition for $\varepsilon$ compels the use of derived boundary conditions, which at best augment numerical stiffness by tying the wall value to derivatives of $k$. A further drawback is that both $k$ and $\varepsilon$ vary as $y^2$ as $y\to0$. The difficulties are discussed by Speziale et al.[1] in connection with a $k$-$\tau$ model, while Shih and Hsu,[2] Lang and Shih,[3] and Rodi and Mansour[4] have used results from direct numerical simulations (DNS) for performance assessment of a number of $k$-$\varepsilon$ variants. Spalding[5] provides a brief recent survey of some possible alternatives to the $k$-$\varepsilon$ model without arriving at an answer to his own question, "which is best ?" The present contribution seeks to demonstrate that there are distinct possibilities in the new $q$-$\zeta$ model.

## The $q$-$\zeta$ Model

**Definition of $q$ and $\zeta$**

The new variables are defined as the square root of the turbulent kinetic energy

$$q\equiv\sqrt{k} \tag{4}$$

and its rate of destruction

$$\zeta\equiv\tilde{\varepsilon}/2q \tag{5}$$

where $\tilde{\varepsilon}$ in Eq. (5) is the isotropic dissipation introduced by Jones and Launder[6] in recognition of the decisive advantages of a dependent variable which is zero at the wall. The drawback is that this use of $\tilde{\varepsilon}$ in the $k$-$\tilde{\varepsilon}$ model entails the calculation of $(\partial q/\partial y)^2$ to recover $\varepsilon$ from

$$\tilde{\varepsilon}=\varepsilon-2\nu\left(\frac{\partial q}{\partial y}\right)^2 \tag{6}$$

This calculation is unnecessary in the $q$-$\zeta$ model. Note that $q$ and $\zeta$ are both $\mathcal{O}(y)$ at the wall.

**$q$ Equation**

An exact equation for $q$ is obtained from the $k$ equation using the identity

$$\frac{\mathrm{D}q}{\mathrm{D}t}\equiv\frac{1}{2q}\frac{\mathrm{D}k}{\mathrm{D}t} \tag{7}$$

The result is

$$U_i\frac{\partial q}{\partial x_i}=\frac{\partial}{\partial x_j}\left\{\nu\frac{\partial q}{\partial x_j}-\overline{u_jq}\right\}-\frac{1}{2q}\frac{\partial}{\partial x_j}\left(\frac{\overline{pu_j}}{\rho}\right)$$
$$-\frac{\overline{u_iu_j}}{2q}\frac{\partial U_i}{\partial x_j}-\frac{\varepsilon}{2q}+\frac{\nu}{q}\frac{\partial q}{\partial x_j}\frac{\partial q}{\partial x_j} \tag{8}$$

Then, to the same level of approximation as Eq. (2)

$$U_i\frac{\partial q}{\partial x_i}=\frac{\partial}{\partial x_j}\left\{\left(\nu+\frac{\nu_t}{\sigma_q}\right)\frac{\partial q}{\partial x_j}\right\}+\frac{P}{2q}-\frac{\tilde{\varepsilon}}{2q} \tag{9}$$

An equation for $q$ had previously been used by Coakley[7] (with vorticity $\omega$ as the second variable). But Coakley's version (as cited in the assessment of Ref. 3) appears not to contain the essential last term in Eq. (8).

**$\zeta$ Equation**

The $\zeta$ equation is obtained from the $q$ and $\varepsilon$ Eqs. (8) and (3) with the aid of

$$\frac{\mathrm{D}}{\mathrm{D}t}\left(\frac{\tilde{\varepsilon}}{2q}\right)\equiv\frac{\zeta}{\tilde{\varepsilon}}\frac{\mathrm{D}\tilde{\varepsilon}}{\mathrm{D}t}-\frac{\zeta}{q}\frac{\mathrm{D}q}{\mathrm{D}t} \tag{10}$$

The result may be condensed to

$$U_i\frac{\partial\zeta}{\partial x_i}=\frac{\partial}{\partial x_j}\left\{\left(\nu+\frac{\nu_t}{\sigma_\zeta}\right)\frac{\partial\zeta}{\partial x_j}\right\}+\left(C_{\varepsilon1}f_{\varepsilon1}-\frac{1}{2}\right)\frac{P\zeta}{q^2}$$
$$-\left(C_{\varepsilon2}f_{\varepsilon2}-\frac{1}{2}\right)\frac{2\zeta^2}{q}+\psi'+\xi' \tag{11}$$

where the constants and functions are those of Eq. (3), $\psi'=\psi/2q$, and $\xi'$ stands for additional, possibly optional, viscous terms.

**$q$-$\zeta$ Model**

Finally, the equations are written in the form

$$U_i\frac{\partial q}{\partial x_i}=\frac{\partial}{\partial x_j}\left\{\left(\nu+\frac{\nu_t}{\sigma_q}\right)\frac{\partial q}{\partial x_j}\right\}+Q-\zeta \tag{12}$$

$$U_i\frac{\partial\zeta}{\partial x_i}=\frac{\partial}{\partial x_j}\left\{\left(\nu+\frac{\nu_t}{\sigma_\zeta}\right)\frac{\partial\zeta}{\partial x_j}\right\}$$
$$+\frac{\zeta}{q}(C_{\zeta1}f_{\zeta1}Q-C_{\zeta2}f_{\zeta2}\zeta)+\psi'+\xi' \tag{13}$$

where $Q$ is the rate of production of $q$

$$Q\equiv\frac{P}{2q}=\gamma_t\frac{\partial U_i}{\partial x_j}\left(\frac{\partial U_i}{\partial x_j}+\frac{\partial U_j}{\partial x_i}\right) \tag{14}$$

$$\gamma_t\equiv\frac{C_\mu f_\mu}{4}\frac{q^2}{\zeta} \tag{15}$$

The production and dissipation damping functions are simply related to those of the $k$-$\varepsilon$ model by $C_\zeta f_\zeta=2C_\varepsilon f_\varepsilon-1$ and the eddy viscosity is

$$\nu_t\equiv C_\mu f_\mu(q^3/2\zeta) \tag{16}$$

Equations (12) and (13) written in this way are very similar to the more familiar $k$ and $\varepsilon$ equations. Thus $P$ and $\varepsilon$ of the $k$ equation have their counterparts $Q$ and $\zeta$ in the $q$ equation and in the eddy-viscosity definition where $k^2/\varepsilon$ is replaced by $q^2/\zeta$. This similarity facilitates the introduction of the new model in computer codes

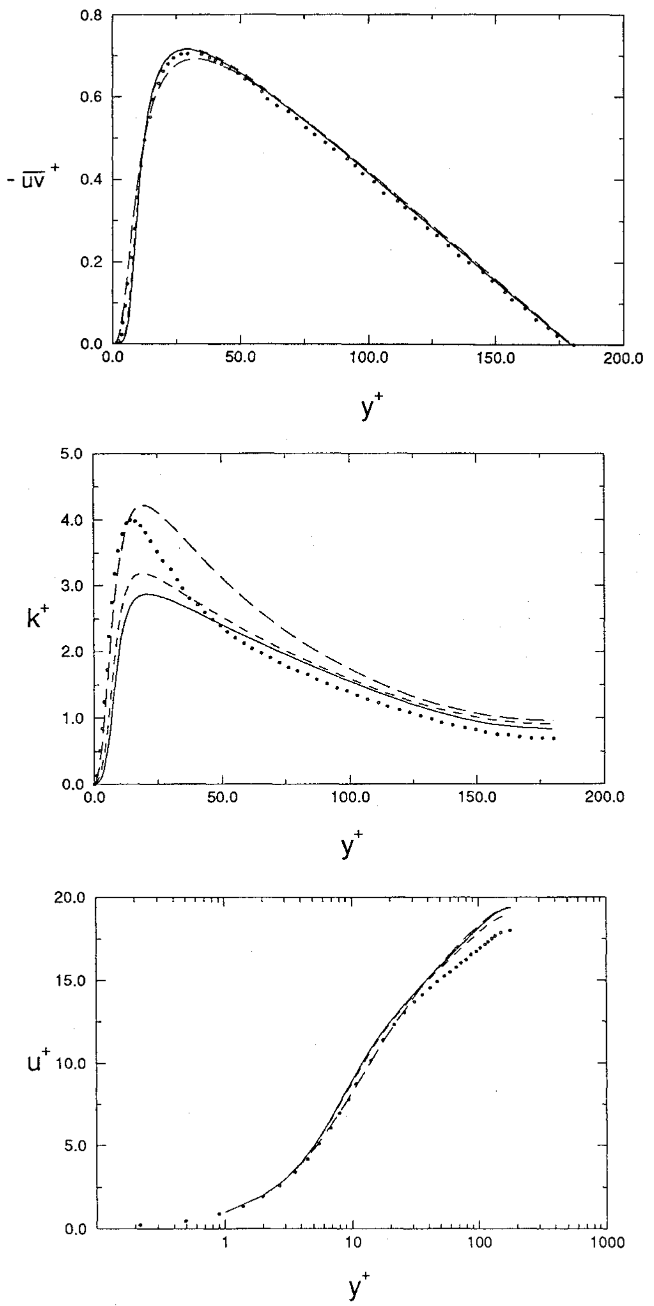


**Fig. 1 Channel-flow predictions compared with DNS results,[11] $Re_\tau$ = 180: · · · DNS, —— $k$-$\tilde{\varepsilon}$ model,[8] - - - $q$-$\zeta$ model (functions of Ref. 8), and — — — $q$-$\zeta$ model (functions of Ref. 9).**

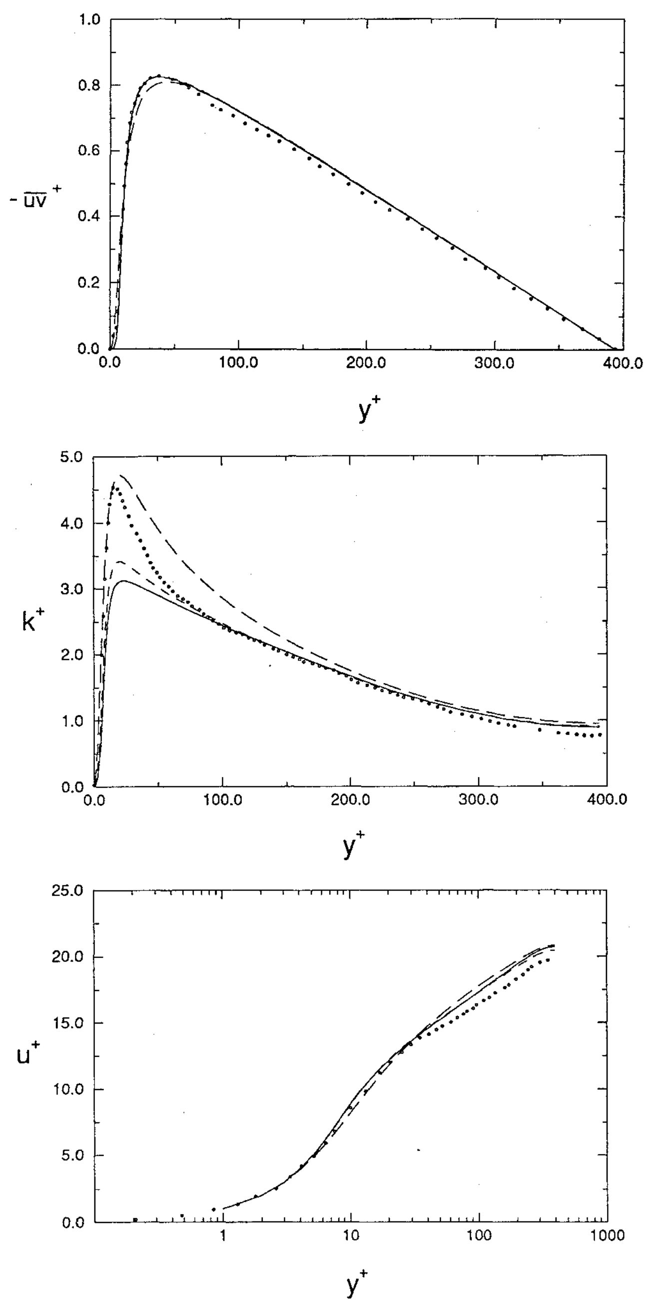


**Fig. 2 Channel-flow predictions compared with DNS results,[11] $Re_\tau$ = 395: symbols as in Fig. 1.**

designed for $k$-$\varepsilon$ calculations. It is easy to show that in the constant-stress logarithmic layer, $-\overline{uv} \approx u_\tau^2$, where $P \approx \varepsilon$ and $Q \approx \zeta$,

$$\frac{u_\tau}{q} = C_\mu^{\frac{1}{4}} \qquad \text{and} \qquad \zeta = \frac{C_\mu^{\frac{1}{4}}}{2}\frac{u_\tau^2}{\kappa y} \tag{17}$$

**Constants and Functions**

The purpose at this stage is not so much to improve the accuracy of the predictions as to test the feasibility of the method, and the derivation of the $q$ and $\zeta$ equations permits the use of established model constants and functions, at least in the first instance. These quantities are to be taken from models based on the $\tilde{\varepsilon}$ equation: that of Jones and Launder[6] in the revised form by Launder and Sharma,[8] and the model of Chien.[9] In the Jones–Launder–Sharma model the local turbulence Reynolds number is the only parameter in the damping functions; Chien's model involves functions expressed in terms of distance from the wall. Therefore, its application to separated flows may be more difficult, but according to Lang and Shih[3] it gives more accurate predictions of two-dimensional channel flow.

Launder and Sharma[8] use the standard high-Reynolds-number $k$-$\varepsilon$ model values: $C_\mu = 0.09$, $C_{\varepsilon 1} = 1.44$, $C_{\varepsilon 2} = 1.92$, $\sigma_q = \sigma_k = 1.0$, and $\sigma_\zeta = \sigma_\varepsilon = 1.3$. Their damping functions for near-wall viscous effects are

$$f_{\varepsilon 1} = 1.0, \qquad f_{\varepsilon 2} = 1 - 0.3\exp\left(\mathrm{Re}_t^2\right),$$
$$f_\mu = \exp\left\{\frac{-3.4}{(1 + \mathrm{Re}_t/50)^2}\right\} \tag{18}$$

For calculations with the $q$-$\zeta$ model the coefficient 3.4 in $f_\mu$ has been replaced by 6.0 to improve predictions of the law of the wall in channel flow. The form of function $f_{\varepsilon 2}$ was originally chosen to fit the decay of isotropic turbulence in the final period. It is negligibly small except very close to the wall, where $\mathrm{Re}_t$ is of order unity, and has little effect on these calculations. It has been necessary to retain the Jones–Launder[6] approximation of the small secondary shear production term, which appears in the $\zeta$ equation as

$$\psi' = 2\nu\gamma_t\left(\frac{\partial^2 U_i}{\partial x_k \partial x_m}\right)\left(\frac{\partial^2 U_i}{\partial x_k \partial x_m}\right) \tag{19}$$

in spite of the finding by Rodi and Mansour[4] that it is at variance with the DNS results. From a practical point of view this model of $\psi'$ is inconvenient in the treatment of anything more complicated than two-dimensional wall flow, and there are strong arguments in favor of omitting it altogether, as do Mansour et al.,[10] and several other authors.

Chien's constants[9] differ slightly from those of the standard $k$-$\varepsilon$ model. They are $C_\mu = 0.09$, $C_{\varepsilon 1} = 1.35$, $C_{\varepsilon 2} = 1.80$, $\sigma_q = \sigma_k = 1.0$, and $\sigma_\zeta = \sigma_\varepsilon = 1.3$. The damping functions are

$$f_{\varepsilon 1} = 1.0, \qquad f_{\varepsilon 2} = 1 - 0.22\exp\left(-\frac{\mathrm{Re}_t^2}{36}\right) \qquad (20)$$
$$f_\mu = 1 - \exp(-0.0115y^+)$$

Chien ignores the secondary shear production of $\tilde{\varepsilon}$ but includes an extra decay term which is inserted in the $\zeta$ equation as

$$\xi' = -\frac{2\nu\zeta}{y^2}\exp\left(-\frac{y^+}{2}\right) \qquad (21)$$

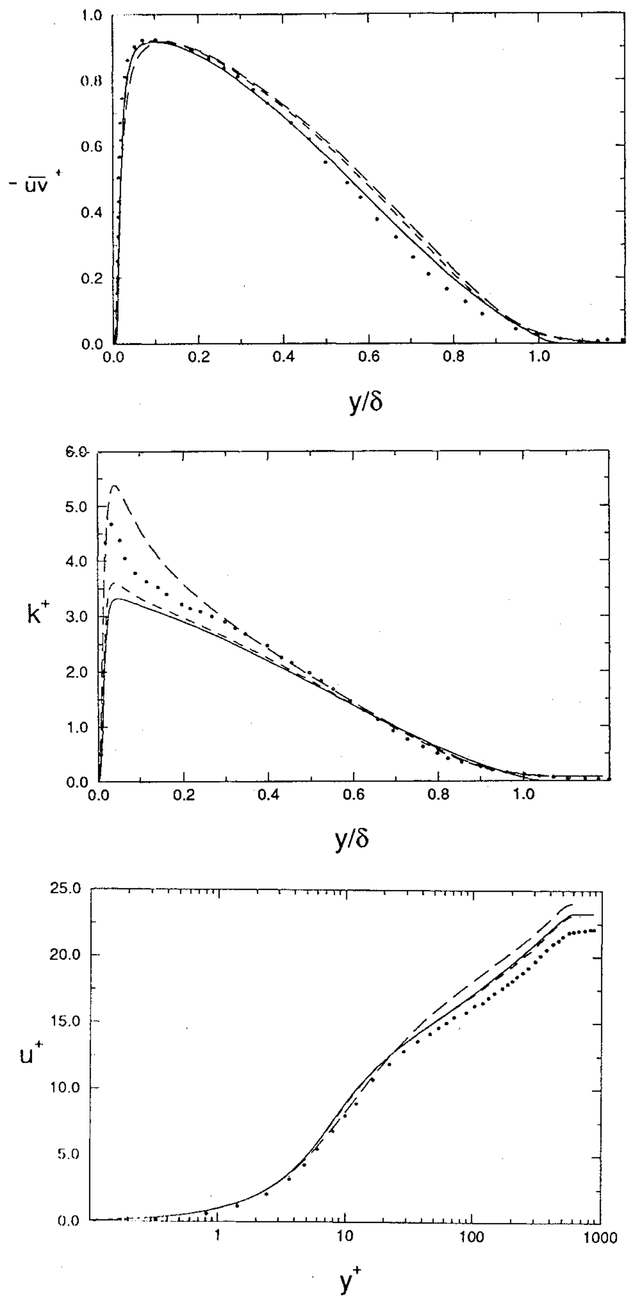


**Fig. 3 Boundary-layer predictions compared with DNS results,[12] $Re_\vartheta$ = 1410: symbols as in Fig. 1.**

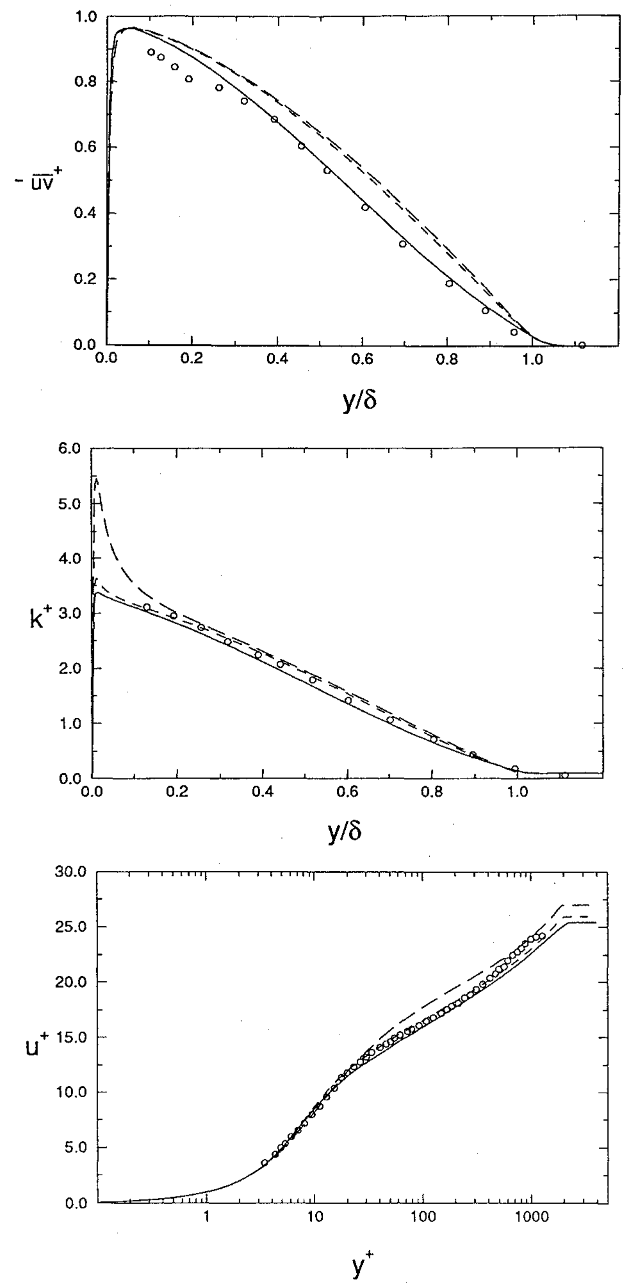


**Fig. 4 Boundary-layer predictions compared with measurements,[13] $Re_\vartheta$ = 5480: o o o, data from Ref. 13, other symbols as in Fig. 1.**

In Eq. (20) $f_\mu$ has the merit of increasing linearly with $y$ as $y \to 0$ to give, correctly, $-\overline{uv} \propto y^3$ near the wall. It also conforms fairly closely to the exact DNS values calculated by Rodi and Mansour[4] and in this respect it is much superior to the corresponding function in Eq. (18).

## Calculations

The first calculations with the new model have been made for comparison with 1) direct numerical simulations[11] of channel flow at $\mathrm{Re}_\tau = 180$ and 395, 2) direct numerical simulation[12] of a boundary layer at momentum thickness Reynolds number $\mathrm{Re}_\vartheta = 1410$, and 3) hot-wire measurements[13] in a boundary layer at $\mathrm{Re}_\vartheta = 5480$. In each case the results obtained from the $q$-$\zeta$ model with alternative sets of damping functions[8,9] are compared with those of the Launder–Sharma[8] $k$-$\varepsilon$ model and with the DNS or experimental data. The channel-flow results were obtained from a one-dimensional finite-volume method by time stepping from assumed initial conditions to the steady-state solution. The boundary-layer calculations were made using a steady-state parabolic matching function.

The results are plotted in Figs. 1–4 in the manner of Ref. 3 so as to facilitate comparison with the performance of other turbulence models discussed therein. The plots show the cross-stream distributions of $U$, $k$, and $-\overline{uv}$ expressed in wall units. The channel-flow results from the $k$-$\tilde{\varepsilon}$ model are identical to those obtained in Ref. 3. They show that the $k$-$\tilde{\varepsilon}$ model fails badly to predict the peak in $k$ obtained from the simulations at $y^+ \approx 20$. The $q$-$\zeta$ model with the Launder–Sharma[8] functions performs a little better in this respect, whereas the use of the Chien functions in this model produces $k^+$ values generally greater than those of the simulations, also in accord with the findings of Ref. 3 for Chien's original model. Although the calculated $\overline{uv}^+$ distributions for the two channel flows agree closely with the DNS results, the mean velocity is rather too high in the logarithmic region. The discrepancy between the calculations and the DNS results is attributable to shortcomings in the viscous-damping functions employed. In this respect the $q$-$\zeta$ model gives typical results. The boundary-layer calculations exhibit broadly the same features; the chief difference being that the agreement with the simulated and measured shear-stress is not as good.

On the whole, the results obtained from the $q$-$\zeta$ models are in no way inferior to those obtained from the established $k$-$\tilde{\varepsilon}$ models considered. But they have been obtained with considerably less computational effort. The superior behavior of $q$ and $\zeta$ in the sublayers permits the use of a relatively coarse grid (in the $\mathrm{Re}_\tau = 395$ channel-flow calculations, 30 cross-stream nodes instead of 40), and the omission of redundant source terms further reduces the computer time required. Grid-independent solutions for the low-Reynolds-number channel flow were obtained in 75% of the CPU time needed for the same calculations with the $k$-$\tilde{\varepsilon}$ model. The saving in CPU time is enhanced when the Reynolds number is increased, to approximately 50% for the boundary-layer calculations at $\mathrm{Re}_\vartheta = 5480$.

## Conclusion

These first results are encouraging but a good deal more needs to be done. Further work should no doubt be concentrated on the formulation of new viscous-layer damping functions in the $\zeta$ equation, with special attention paid to the constraints imposed by the need for consistent boundary conditions at the wall. For the present calculations we have been content to borrow functions from established $k$-$\varepsilon$ models as a temporary expedient. The present short paper is intended only to draw attention to the possibilities.

## Acknowledgment

We gratefully acknowledge financial support for A. A. Dafa'Alla from the Engineering and Physical Sciences Research Council.

## References

[1]Speziale, C. G., Abid, R., and Anderson, E. C., "Critical Evaluation of Two-Equation Models for Near-Wall Turbulence," *AIAA Journal*, Vol. 30, No. 2, 1992, pp. 324–331.

[2]Shih, T.-H., and Hsu, A. T., "An Improved $k$-$\varepsilon$ Model for Near-Wall Turbulence," AIAA Paper 91-0611, 1991.

[3]Lang, N. J., and Shih, T.-H., "A Critical Comparison of Two-Equation Turbulence Models," NASA TM 105237, ICOMP-91-15, 1991.

[4]Rodi, W., and Mansour, N. N., "Low Reynolds Number $k$-$\varepsilon$ Modelling with the Aid of Direct Simulation Data," *Journal of Fluid Mechanics*, Vol. 250, 1993, pp. 509–529.

[5]Spalding, D. B., "Kolmogorov's Two-Equation Model of Turbulence," *Proceedings of the Royal Society Ser. A*, Vol. 434, 1991, pp. 211–216.

[6]Jones, W. P., and Launder, B. E., "The Prediction of Laminarization with a Two-Equation Model of Turbulence," *International Journal of Heat and Mass Transfer*, Vol. 15, No. 2, 1972, pp. 301–313.

[7]Coakley, T. J., "Turbulence Modelling Methods for the Compressible Navier-Stokes Equations," AIAA Paper 83-1693, 1983.

[8]Launder, B. E., and Sharma, B. I., "Application of the Energy-Dissipation Model of Turbulence to the Calculation of the Flow near a Spinning Disk," *Letters in Heat and Mass Transfer*, Vol. 1, No. 1, 1974, pp. 131–138.

[9]Chien, K.-Y., "Predictions of Channel and Boundary Layer Flows with a Low-Reynolds-Number Turbulence Model," *AIAA Journal*, Vol. 20, No. 1, 1982, pp. 33–38.

[10]Mansour, N. N., Kim, J., and Moin, P., "Near-Wall $k$-$\varepsilon$ Modeling," *AIAA Journal*, Vol. 27, No. 8, 1989, pp. 1068–1073.

[11]Kim, J., Moin, P., and Moser, R., "Turbulence Statistics in Fully Developed Channel Flow at Low Reynolds Number," *Journal of Fluid Mechanics*, Vol. 177, 1987, pp. 133–166.

[12]Spalart, P. R., "Direct Simulation of a Turbulent Boundary Layer up to $R_\vartheta = 1410$," *Journal of Fluid Mechanics*, Vol. 187, 1988, pp. 61–98.

[13]Gibson, M. M., Verriopoulos, C. A., and Vlachos, N. S., "Turbulent Boundary Layer on Mildly Curved Convex Surface: 1 Mean Flow and Turbulence Measurements," *Experiments in Fluids*, Vol. 2, No. 1, 1984, pp. 17–24.

# Computation of Compression Ramp Flow with a Cross-Diffusion Modified $k$–$\varepsilon$ Model

Byong Kuk Yoon* and Myung Kyoon Chung†
*Korea Advanced Institute of Science and Technology, Taejon 305-701, Republic of Korea*

## Introduction

SINCE the advent of the standard $k$–$\varepsilon$ model, it has been very widely accepted as a quite dependable turbulence model in engineering field. Numerous tests however, have revealed its shortcomings in predicting nonequilibrium flows, such as the shock-wave/turbulent boundary-layer interaction flow over a ramp. In contrast, the $k$–$\omega$ model of Wilcox[1] produces significantly better skin friction distribution than the $k$–$\varepsilon$ model for such nonequilibrium flows. Wilcox[2] attributed the better performance of the $k$–$\omega$ model to a cross diffusion between $k$ and $\varepsilon$ implicitly contained in the $\omega$ equation; $k$ and $\varepsilon$ which determine the turbulence length scale near the wall under a nonnegligible pressure gradient are strongly interdependent on each other.

Actually, it was shown by Leslie[3] with a statistical analysis that the turbulent transport term in the $k$ equation depends on both gradient diffusions of $k$ and $\varepsilon$. However, it has not been fully examined whether the cross-diffusion term should indeed be included in the conventional $k$–$\varepsilon$ model or not. This Note is aimed at proposing a new $k$–$\varepsilon$ model with a cross-diffusion term that can be used to analyze turbulent nonequilibrium flows.

## Model Equations

Most extensive turbulent diffusion models for $k$ and $\varepsilon$ equations have been derived by Yoshizawa[4] with the two-scale direct-interaction approximation (TSDIA) as follows:

$$T_k = \frac{\partial}{\partial x_j}\left(C_{kk}C_\mu\frac{k^2}{\varepsilon}\frac{\partial k}{\partial x_j}\right) + \frac{\partial}{\partial x_j}\left(C_k C_\mu\frac{k^3}{\varepsilon^2}\frac{\partial \varepsilon}{\partial x_j}\right) \tag{1}$$

$$T_\varepsilon = \frac{\partial}{\partial x_j}\left(C_{\varepsilon\varepsilon}C_\mu\frac{k^2}{\varepsilon}\frac{\partial \varepsilon}{\partial x_j}\right) + C_\mu\left[\frac{\partial}{\partial x_j}\left(C_{\varepsilon k}k\frac{\partial k}{\partial x_j}\right) + C'_{\varepsilon 1}\left(\frac{\partial k}{\partial x_j}\right)^2 + C'_{\varepsilon 2}\frac{k}{\varepsilon}\frac{\partial k}{\partial x_j}\frac{\partial \varepsilon}{\partial x_j} + C'_{\varepsilon 3}\frac{k^2}{\varepsilon^2}\left(\frac{\partial \varepsilon}{\partial x_j}\right)^2\right] \tag{2}$$

where $C_{kk}$, $C_{\varepsilon\varepsilon}$, $C_{k\varepsilon}$, $C_{\varepsilon k}$, $C'_{\varepsilon 1}$, $C'_{\varepsilon 2}$, and $C'_{\varepsilon 3}$ are model constants. Note that the conventional $k$–$\varepsilon$ model adopts the first terms only in these models. Because of the plethora of the model constants, however, they have not been further pursued in practical applications.

Received Nov. 29, 1994; revision received March 14, 1995; accepted for publication March 14, 1995. 

*Graduate Research Assistant, Department of Mechanical Engineering, Yusong-ku.

†Professor, Department of Mechanical Engineering, Yusong-ku.